



University of Groningen

Monolayer Superconductivity in WS₂

Zheliuk, Oleksandr; Lu, Jianming; Yang, Jie; Ye, Jianting

Published in:

Physica status solidi-Rapid research letters

DOI:

[10.1002/pssr.201700245](https://doi.org/10.1002/pssr.201700245)

IMPORTANT NOTE: You are advised to consult the publisher's version (publisher's PDF) if you wish to cite from it. Please check the document version below.

Document Version

Final author's version (accepted by publisher, after peer review)

Publication date:

2017

[Link to publication in University of Groningen/UMCG research database](#)

Citation for published version (APA):

Zheliuk, O., Lu, J., Yang, J., & Ye, J. (2017). Monolayer Superconductivity in WS₂. Physica status solidi-Rapid research letters, 11(9), [1700245]. <https://doi.org/10.1002/pssr.201700245>

Copyright

Other than for strictly personal use, it is not permitted to download or to forward/distribute the text or part of it without the consent of the author(s) and/or copyright holder(s), unless the work is under an open content license (like Creative Commons).

Take-down policy

If you believe that this document breaches copyright please contact us providing details, and we will remove access to the work immediately and investigate your claim.

Downloaded from the University of Groningen/UMCG research database (Pure): <http://www.rug.nl/research/portal>. For technical reasons the number of authors shown on this cover page is limited to 10 maximum.

Monolayer superconductivity in WS₂

Oleksandr Zheliuk, Jianming Lu, Jie Yang and Jianting Ye*

Zernike Institute for Advanced Materials, University of Groningen, Nijenbourgh 4, 9747AG, Groningen, Netherlands

Keywords monolayer superconductivity, transition metal dichalcogenides, chemical vapor deposition.

* Corresponding author: e-mail j.ye@rug.nl, Phone: +31 50 36 34376, Fax: +31 50 36 34441

Superconductivity in monolayer tungsten disulfide (2H-WS₂) is achieved by strong electrostatic electron doping of electric double-layer transistor (EDLT). Single crystals of WS₂ are grown by scalable method – chemical vapor deposition (CVD) on standard Si/SiO₂ substrate. Monolayers are identified by both AFM and color-coding tech-

niques. ELDT device based on single layer WS₂ shows ambipolar transfer characteristics indicating semiconducting nature of material. Metallic transport in electron side evolves into superconductor with critical temperature $T_C = 3.15$ K.

Copyright line will be provided by the publisher

1 Introduction Semiconducting Transition metal dichalcogenides (TMD) such as MoS₂, MoSe₂, WS₂, and WSe₂ are known candidate for two-dimensional (2D) electronics due to their layered composition and unique band structure, which undergoes indirect to direct band gap transition when exfoliated down to the monolayer. The absence of inversion symmetry in monolayer hexagonal lattice together with strong spin-orbit interaction coming from heavy transition metal ion leads to a lifted spin degeneracy near the band edges, making this material a testing platform of various phenomena of solid state physics [1,2].

Superconductivity is known to exist in alkali metal intercalated bulk MoS₂ with T_C up to 7.3 K [3]. Recently discovered electrostatically induced superconductivity in multilayer MoS₂ flakes paves a way to more controllable superconducting devices, where T_C can be electrically tuned from 0 to 10 K [4]. A similar technique has been used to induce superconducting state on the surface of bulk WS₂ with $T_C \sim 2$ K at half of normal resistance $R_N^{50\%}$ [5]. Such a state is believed to originate from the top most layer and show the properties of true 2D superconductor such as BKT transition, coherence length larger than superconductor thickness, the high anisotropy of upper critical field with pronounced cusp shape. Among others unique properties, primarily, electrons of spin-polarized Cooper pairs residing at K and K' valleys makes TMDs highly resilient against applied in-plane magnetic field [6].

In most transport studies of TMDs on ultrathin flakes, samples were prepared by mechanical exfoliation from bulk. Another approach is to use chemical vapor deposition (CVD) growth to obtain ultrathin flakes down to single layer. Widely developed for TMD materials, CVD technique allows obtaining monolayer single crystal domains

with a lateral size of 20–100 μm , which can be easily accessed by standard microfabrication processes. However, the quality of crystalline monolayer prepared by CVD is usually expected to be lower than the mechanically exfoliated ones making CVD samples less studied for their basic physical properties.

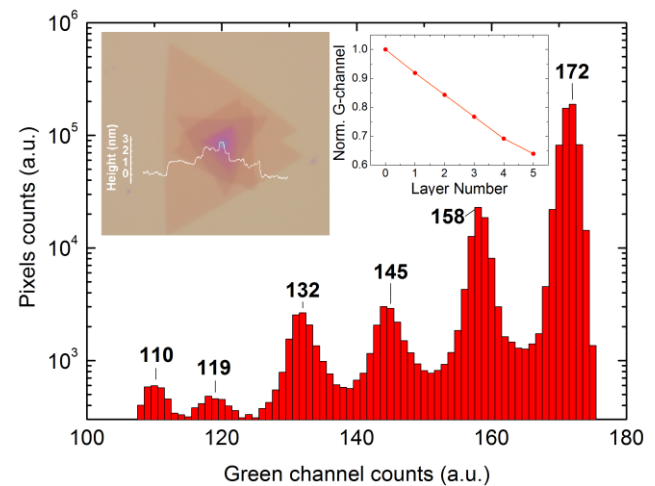


Figure 1 Layer number identification of CVD grown WS₂ by color coding technique. Sample area plotted as a function of reflected intensity (represented by pixel count and green channel counts respectively). Peak with the largest number of counts corresponds to the reflection from the bare substrate. *Top left inset:* optical image of multilayer WS₂ flake and AFM profile measured across the sample. *Top right inset:* number of green channel counts normalized with respect to bare substrate counts plotted against layer number.

2 Results

Copyright line will be provided by the publisher

Typical multilayer WS₂ grown by CVD method is shown in the inset of Fig.1. Steps corresponding to different layer number can be clearly resolved in AFM profile scan. Here, the thickness of each layer is 0.6 nm and the bottom layer together with Van der Waals gap against the substrate is ~1 nm (due to an asymmetric environment) consistent with previous reports [7]. The number of layers can be determined consistently by color coding technique, which is alternative technique suitable for ultrathin layered 2D materials on flat substrates such as Si/SiO₂.

The histogram represents sample area (in pixel counts) as a function of reflected intensity on the green channel of CCD. Peak with the highest area as well as highest reflected intensity corresponds to a bare Si/SiO₂ substrate reflection. Next peak at 158 counts corresponds to the reflection from the monolayer, reflection from each next layer reduces total intensity by 7.4%. The normalized intensity of reflection on the green channel as a function of layer number shows linear decrease up to 5 layers (see right inset of Fig.1). It shows saturating dependence when the number of layers increases further.

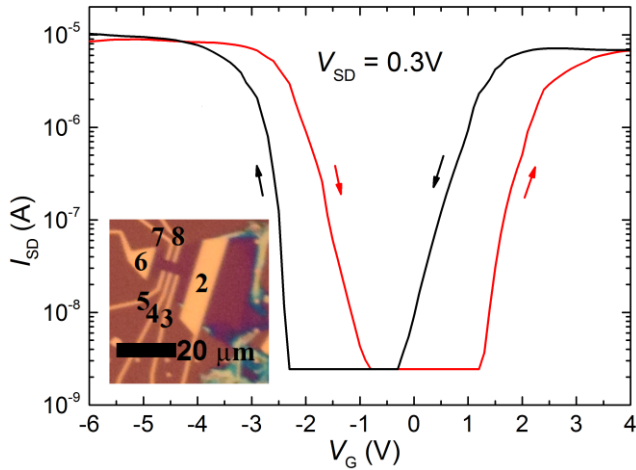


Figure 2 Transfer characteristics of EDLT device based on monolayer WS₂. Arrows indicate the direction of gate voltage sweep. *Inset*: optical image of the typical device structure.

Large area single layer WS₂ flakes were selected for device fabrication. Standard e-beam lithography defines electrodes composed of 5/50 nm of Ti/Au. Before measurement, the sample was covered with a small droplet of ionic liquid: DEME-TFSI. The transfer curve measured at 220 K is shown in Fig. 2. Both valence and conduction band transport can be accessed within gate bias $V_G = \pm 4$ V range with on current reaching 10 and 6 μ A for accumulating holes and electrons, respectively. Hysteresis in the order of 1.5 V observed during measurement is caused by reduced ion mobility at 220K. Insulating regime spans around 2V consistent with a direct band gap of monolayer WS₂. At $V_G = 0$ V devices are usually insulating indicating high crystallinity and absence of charged impurities. Re-

peatability was found for most of the devices indicating chemical stability within the electrochemical window of ± 4 V.

Keeping the gate voltage constant, the sample was cooled below glass transition temperature of the ionic liquid (~190K) with 3K/min to ensure the fast freezing of ion movement. When temperature reached below 170 K gate voltage was set to $V_G = 0$ without losing the induced electronic state.

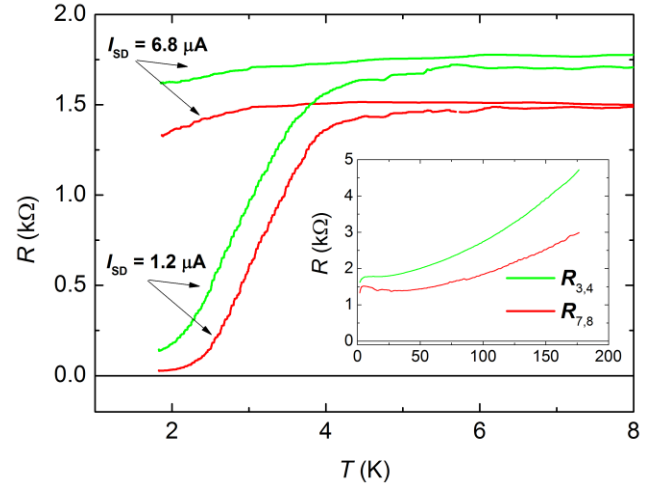


Figure 3 Resistance of monolayer WS₂ as a function of temperature close to superconducting transition. Contact leads 3-4 and 7-8 are probing different sample region (numbers correspond to those in Fig.2.). Upper and lower set of data corresponds to high (6.8 μ A) and low (1.2 μ A) excitation current. *Inset*: resistance measured up to high temperatures.

The resistances of probes 3-4 and 7-8 measured as a function of temperature are shown in Fig. 3. Overall sample shows metallic behavior down to low temperature, where normal resistance reaches 1.4 and 1.8 k Ω for a different channel. Both channels undergo superconducting transition below 4K, which can be clearly resolved when the excitation current is reduced from 6.8 to 1.2 μ A. (Fig. 3). Slight difference in T_C is attributed to the spatial variation of doping level across the sample surface. It is interesting to note that $T_C = 3.15$ K is higher than achieved by a similar method in bulk WS₂ crystals [5].

Large magnetoresistance below transition temperature confirms the presence of the superconducting state in monolayer WS₂. As shown in Fig. 4, the perpendicular critical field B_{C2}^\perp increases linearly with the lowering of sample temperature. The B_{C2}^\perp obtained by $R_N^{50\%}$ criteria reaches ~1.05 T by extrapolation to zero temperature similar to that found in monolayer MoS₂ [8]. From the linear dependence of B_{C2}^\perp which is consistent with the standard linearized Ginzburg-Landau theory, we estimate the superconducting coherence length $\xi_{GL} = 17.7$ nm which is much larger than the 0.6 nm thick monolayer and confirms formation of a 2D superconducting state in monolayer WS₂.

3 Conclusions Here we reported the first observation of superconducting state in CVD grown WS₂ monolayer crystal, which is industrially friendly and air stable semiconducting material. Surprisingly, critical temperature $T_c = 3.15\text{ K}$ is higher than in its bulk counterpart indicating CVD-grown monolayer shows at least similar sample quality as compared to the samples prepared by mechanical exfoliation.

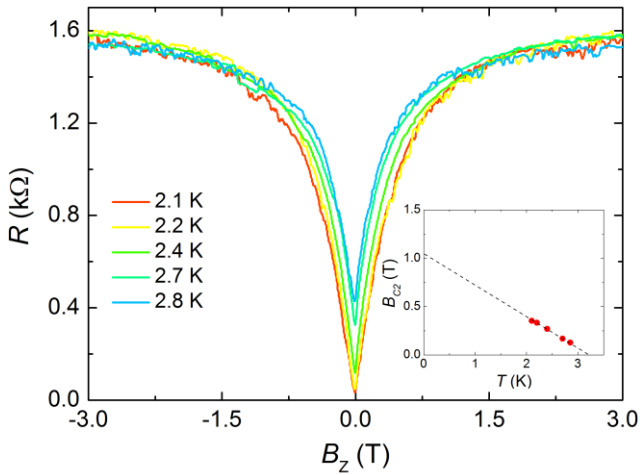


Figure 4 Resistance of WS₂ superconductor under perpendicular magnetic field from -3 T to 3 T. Each curve corresponds to the sample at different temperatures ranging from 2.1 K to 2.8 K. *Inset:* critical field as a function of temperature.

Acknowledgments We thank J. Harkema for technical support. This work is financially supported by the European Research Council (consolidator grant no. 648855 Ig-QPD).

References

- [1] K. F. Mak, J. Shan, Nat. Photon. 10, 216-226 (2016).
- [2] X. Xu, W. Yao, D. Xiao, T. F. Heinz, Nat. Phys., 10, 343-350 (2014).
- [3] J. A. Woollam, R. B. Somoano, Phys. Rev. B 13, 3843-3853 (1976).
- [4] J. T. Ye, Y. J. Zhang, R. Akashi, M. S. Bahramy, R. Arita, Y. Iwasa, Science 338, 1193-1196 (2012).
- [5] S. Jo, D. Constanzo, H. Berger, A. Morpurgo, Nano Lett., 15(2), 1197-1202 (2015).
- [6] J. M. Lu, O. Zheliuk, I. Leermakers, N. F. Q. Yuan, U. Zeitler, K. T. Law, and J. T. Ye, Science 350, 1353 (2015).
- [7] J. Park, W. Lee, T. Choi, S.-H. Hwang, J. M. Myong, J.-H. Jung, S.-H. Kim, H. Kim, Nanoscale 7, 1308-1313 (2015).
- [8] D. Constanzo, S. Jo, H. Berger, A. Morpurgo, Nat. Nanotechnol. 11, 339-344 (2016). [a] X. Xu, W. Yao, D. Xiao, T. F. Heinz, Nat. Phys., 10, 343-350 (2014).